JULY 30 2003

The predicted barrier effects in the proximity of tall buildings

Kai Ming Li; Siu Hong Tang

J. Acoust. Soc. Am. 114, 821–832 (2003)
https://doi.org/10.1121/1.1593060

The predicted barrier effects in the proximity of tall buildings

Kai Ming Li[a] and Siu Hong Tang
Department of Mechanical Engineering, The Hong Kong Polytechnic University, Hung Hom, Kowloon, Hong Kong

(Received 27 November 2002; revised 18 May 2003; accepted 30 May 2003)

A ray model is developed and validated for the prediction of the insertion loss of barriers that are placed in front of a tall building in high-rise cities. The model is based on the theory of geometrical acoustics for sound diffraction at the edge of a barrier and multiple reflections by the barrier and façade surfaces. It is crucial to include the diffraction and multiple reflection effects in the ray model, as they play important roles in determining the overall sound pressure levels for receivers located between the façade and barrier. Comparisons of the ray model with indoor experimental data and wave-based boundary element formulation show reasonably good agreement over a broad frequency range. Case studies are also presented that highlight the significance of positioning the barrier relative to the noise-sensitive receivers in order to achieve improved shielding efficiency of the barrier. © *2003 Acoustical Society of America.* [DOI: 10.1121/1.1593060]

PACS numbers: 43.50.Gf, 43.28.En, 43.50.Rq [DKW]

I. INTRODUCTION

The use of acoustic barriers to shield land transportation noise sources from neighborhood residents has been implemented extensively in many countries worldwide. Since the late 1960s,[1–6] much effort has been put into predicting the sound levels behind barriers by using theoretical studies, scaled-model experiments, and other more costly full-scale field experiments. Despite this widespread interest, there are relatively few studies that consider the barrier effect on the overall sound pressure levels in front of a tall building. This typical urban scenario is particularly important in high-rise cities where noise barriers are sometimes built close to tall residential buildings.

In the absence of other reflecting surfaces, diffraction over the top edge is often the only path for sound waves to reach receivers located at the opposite side of the barrier. In this simplest case, rules and charts are available to aid the practical design of noise barriers such that their acoustic performance can be assessed readily. Theoretical approximations and field experience were combined heuristically to devise these design rules and charts.[4,7,8] Much of this early theoretical work on the study of noise barriers was based on the classical diffraction theory.[9] More recent theoretical work has allowed the presence of the impedance ground, the use of sound-absorbent materials on the barrier surface, and multiple diffraction/reflection between two barriers.[10–12] However, with a barrier situated in front of a tall building, a series of image sources are formed behind the façade and barrier surfaces due to multiple reflections. Most standard prediction methodologies, for example, the CRTN[13] and FHWA programs,[14] do not take into account the prediction of the sound field due to these multiple reflections occurring between a façade–barrier system.

Sakurai *et al.*[15] used a time–domain method to investigate the sound field of the façade–barrier system. The prediction of the sound field around the barrier was based on the Kirchhoff–Rubinowicz theory but their theoretical model was not in accord with their experimental data for sound fields measured behind the barrier. Walerian *et al.*[16] developed a computer simulation program to evaluate the time-averaging sound pressure levels in an outdoor environment. However, their program involved too many different parameters, which made it somewhat complex to apply in the present façade–barrier system.

Cheng and Ng[17] studied the acoustic performance of a parallel barrier in front of a building façade. They used an empirical diffraction model but they did not consider the multiple reflections between the façade and barrier and only one image source was included in their numerical formulation. Godinho *et al.*[18] used the boundary element method (BEM) to determine the sound field produced by an infinitely long barrier in the vicinity of building façades. The BEM numerical scheme is an accurate numerical method. One of its main disadvantages is that it is very computationally intensive, especially at high frequencies. In Godinho's investigations, no experiments were conducted, but they compared their numerical results with those obtained by other rather simplified prediction models.[14,19] These simplified models were mainly used for outdoor situations and did not show much agreement with their BEM results.

In this paper, we aim to develop a ray-based model for the prediction of the effect of a noise barrier in the vicinity of tall buildings. The theoretical formulation for the ray model is outlined in Sec. II. Details of numerical and indoor experiments for the validation of the theoretical model are presented in Sec. III. In Sec. IV, typical outdoor situations are simulated that investigate the façade effect on the acoustic performance of noise barriers. Concluding remarks are offered in Sec. V.

II. THEORY—FORMULATION OF A RAY MODEL

We consider a typical scenario of a high-rise city in which a noise barrier of height H is aligned parallel to a row

[a]Author to whom correspondence should be addressed. Electronic mail: mmkmli@polyu.edu.hk

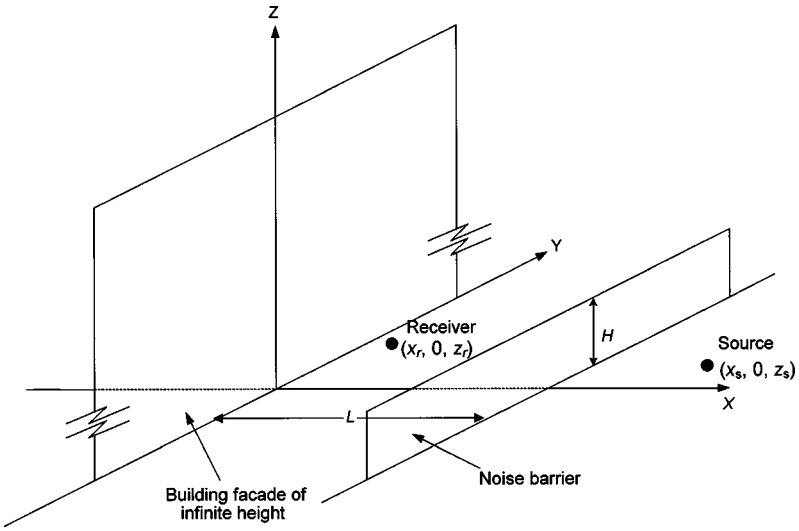

FIG. 1. Schematic diagram of the source/receiver configuration in a façade–barrier system.

of tall buildings. The barrier is designed to shield residents in the buildings from noise sources that are located on the opposite side of the barrier. To model the problem, we assume that the tall buildings are replaced by a plane façade where the barrier is built at a distance L in front of it, above an absorbing ground. Figure 1 shows a schematic diagram of the specified problem. The façade is situated along the y axis at the $x=0$ plane. Furthermore, the façade is assumed to be much higher than the barrier and receiver so that diffraction of sound at the top of the façade can be ignored. We are primarily interested in a three-dimensional problem where the barrier and building façade are placed on the ground surface at the plane of $z=0$. They are extended to infinity in both directions along the y axis, i.e., $-\infty \leqslant y \leqslant +\infty$, so that sound diffracted at their side edges is omitted. To simplify the problem, let the source and receiver be located at the same vertical plane at $y=0$. A time-dependent factor $e^{-i\omega t}$ is understood in this paper.

A rectangular coordinate system is used where the receiver is positioned at $\mathfrak{R} \equiv (x_r,0,z_r)$ between the barrier and façade. A noise source is placed on the opposite side of the barrier at $\Psi_0 \equiv (x_s,0,z_s)$, where $x_s \geqslant L$ and z_s, $z_r \geqslant 0$. Using the image source concept, an image source above the impedance boundary at $\Psi_0' \equiv (x_s,0,-z_s)$ can be identified immediately. In the present study, we wish to investigate the case where the receivers are located in front of the façade but are separated from the source by the barrier, i.e., $L \geqslant x_r \geqslant 0$. Let us consider a more general situation where the ground surfaces have the specific normalized admittance of β_1 at the receiver side and β_2 at the source side. Since acoustically hard materials are commonly used for the façade and barrier surfaces in most metropolitan areas, the specific normalized admittance of the façade and barrier surfaces are assumed to be zero.

When the barrier blocks the direct line-of-sight contact between the receiver and noise source, the receiver itself is located in the shadow zone. In this case, the diffraction of sound at the top edge of the barrier is the only transmission path for the propagation of noise toward the receiver, as the transmission of sound through the barrier is ignored. On reaching the top edge of the barrier, part of the diffracted waves propagate toward the receiver directly. Other parts of the diffracted waves are reflected at the ground and façade surfaces before they reach the receiver. The point of diffraction at the barrier edge, which is located at H above the ground surface, may be treated as a secondary noise source. Since this secondary noise source is located at the top edge of the barrier's surface, multiple reflections take place between the façade and barrier before the diffracted waves arrive at the reception point. Images of the primary and secondary sources are formed in the quarters of $x>0$, $z>0$ and $x<0$, $z>0$. By virtue of the impedance boundary, ground-reflected image sources are also formed in the quarters of $x<0$, $z<0$ and $x>0$, $z<0$. The positions of these primary and secondary sources and their corresponding images can be identified as located at $\Psi_n=(x_n,0,z_s)$, $\mathbf{S}_n=(\overline{x_n},0,H)$, $\Psi_n'=(x_n,0,-z_s)$, and $\mathbf{S}_n'=(\overline{x_n},0,-H)$, respectively. Here, n is the order of the image sources that can be regarded as the number of reflections from the two parallel surfaces. When the order n is an odd number (equal to $2m+1$, say), the image source is located at the left side behind the façade surface ($x<0$). In this particular image source, the ray can be identified as hitting the façade surface $m+1$ times and interacting with the barrier surface m times. When n is even, the image source is situated at the right side behind the barrier surface ($x>0$). The corresponding ray will hit the façade and barrier surfaces an equal number of times. In addition, an extra reflection occurs for those image sources located below the ground surface.

A close examination of the positions of the secondary source and its images reveals that the distance in the x direction of the consecutive images in each quarter differs by a length of $2L$. It is straightforward to generalize the x coordinate, x_n of the secondary source and its images. It is interesting to note that the even- and odd-order rays (order $2m$ and $2m+1$ for $m=0,1,2,...$) are of equal horizontal distance from the origin:

$$\begin{aligned} x_{2m} &= -x_{2m+1} = (2m+1)x_s, \\ \overline{x}_{2m} &= -\overline{x}_{2m+1} = (2m+1)L, \end{aligned} \quad \text{for } m=0,1,2,3,\ldots. \tag{1}$$

A negative sign is required for the x coordinates of all odd-

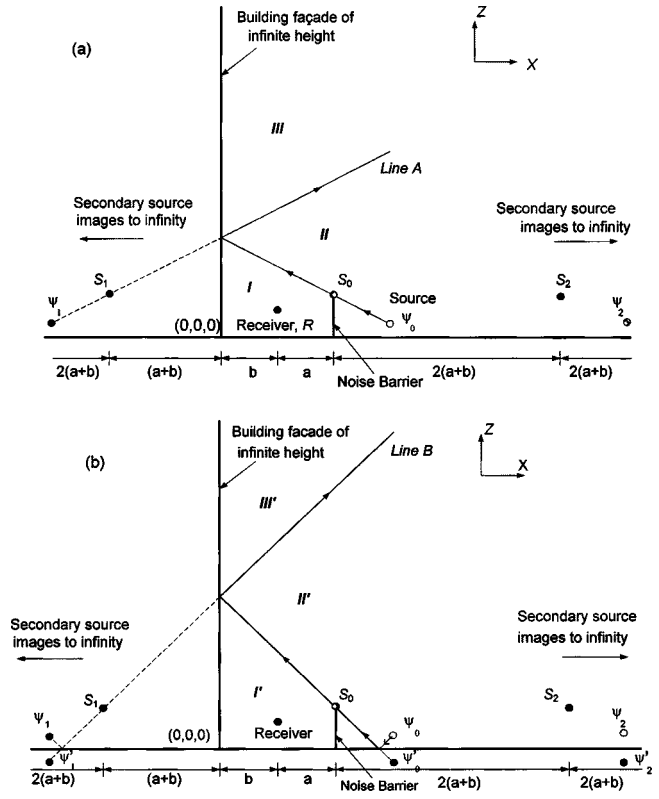

FIG. 2. The source/receiver geometry in a façade–barrier system in the x-z plane. The distance between the receiver and barrier is denoted as "a." The distance between the receiver and building façade is denoted as "b." Subsequent secondary source images are separated by a distance of $2(a+b)$. The three regions of the sound field are formed by (a) the primary noise source, ψ_0; and (b) the image source, ψ_0', due to the reflection from the ground.

order rays because these sources are located at the left side behind the façade surface ($x<0$).

The geometrical configuration of the problem is shown in Fig. 2(a), illustrating the positions of receiver, primary noise source, secondary noise source, and its images in the $x-z$ plane. For reasons of clarity, the image sources below ground are not shown in Fig. 2(a). In principle, the number of images tends to infinity as they line up in the $\pm x$ directions. However, in practice, only a finite number of image sources contribute to yield the total sound field. Obviously, if the separation between the barrier and façade is smaller, more image sources will be generated within a specified distance because of the increased number of possible reflections between these two vertical surfaces. This may lead to a more intense noise level as more image sources contribute to the total sound field. We reiterate that both source and receiver are assumed to locate at the same vertical plane at $y=0$ and the primary source is located below the barrier top edge, but the receiver is allowed to vary along the height of the façade above the barrier top edge. This arrangement permits us to simulate situations where the noise-sensitive receivers reside on different floors in the buildings.

Let us investigate different zones of the sound field in the proximity of the façade–barrier system. The current setup is quite complicated due to the presence of a building façade behind the noise barrier. When a receiver is located in the shadow zone [i.e., Region I of Fig. 2(a)], the line of sight between the source and receiver is blocked. The sound field is mainly dominated by the diffracted waves and their subsequent multiple reflections between the façade and barrier surfaces. An image source method, see, for example, Ref. 20, is used to account for the effects of multiple reflections. According to this concept, each reflected wave is replaced by a wave emitted from an image source. In Region I, the total sound field is determined by summing all diffraction terms formed by these secondary image sources. To compute the diffracted wave terms, it is useful to consider the geometrical configuration, as shown in Fig. 3(a). For a point source located at $\Psi_0 \equiv (x_s,0,z_s)$, receiver at $\Re \equiv (x_r,0,z_r)$, and the point of diffraction at $\mathbf{D} \equiv (x_d,0,z_d)$, Pierce's formulation[21] may be used to compute the diffracted sound field by using the following formula:

$$P(\mathbf{S},\Re,\mathbf{D}) = \left(\frac{e^{i\pi/4}}{\sqrt{2}}\right)\left[\frac{e^{ik(d_S+d_R)}}{4\pi(d_S+d_R)}\right] \times [A_D(X_+)+A_D(X_-)], \tag{2}$$

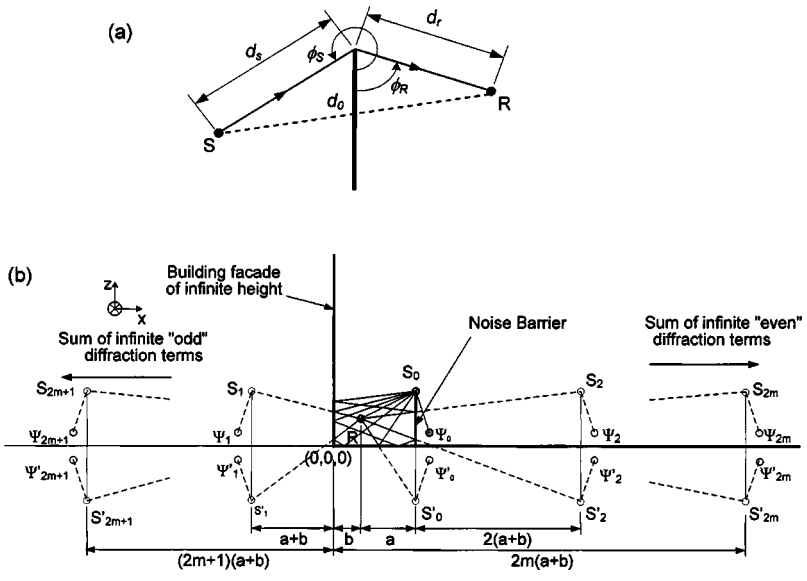

FIG. 3. (a) The geometrical configuration for the diffraction of sound by a thin barrier. (b) Schematic diagram showing multiple reflections between the façade and barrier surfaces for the receiver height is less than that of the barrier.

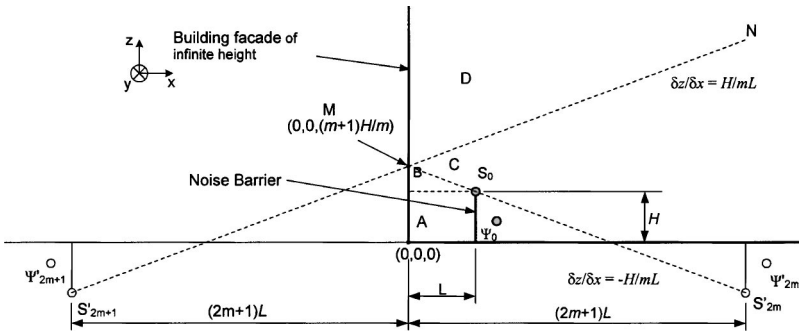

FIG. 4. The source/receiver geometry in a façade–barrier system in the x-z plane. Four different regions A, B, C, and D, are identified due to positions of the diffraction edge and the images of the even and odd virtual sources, S_{2m} and S'_{2m}.

where d_S and d_R are the respective distances from the source and receiver to the diffraction point. The function, $A_D(X)$, is the diffraction integral[21] given by

$$A_D(X)=\mathrm{sgn}(X)[f(|X|)-ig(|X|)], \tag{3}$$

where sgn(X) is the sign function, and $f(X)$ and $g(X)$ are the auxiliary Fresnel functions[22] of real argument X. The arguments of the diffraction integral, X_+ and X_-, are determined by

$$X_\pm=X(\phi_R\pm\phi_S), \tag{4}$$

where

$$X(\Phi)=\left[-2\cos\left(\frac{\Phi}{2}\right)\right]\sqrt{\frac{2\cdot d_S\cdot d_R}{\lambda(d_S+d_R)}}, \tag{5}$$

λ is the wavelength of the diffracted sound, and the angles ϕ_R and ϕ_S are defined in the surface of the screen, as shown in Fig. 3(a). The argument Φ in Eq. (5) is either $(\phi_R+\phi_S)$ or $(\phi_R-\phi_S)$ for X_+ and X_-, respectively.

The total diffracted sound field due to the primary sources can be calculated as follows:

$$P_D=P_A+P_B \tag{6a}$$

where P_A and P_B are corresponding contributions from the secondary sources (even- and odd-order image sources, respectively) above and below the ground surfaces. They are determined by

$$P_A=\sum_m Q(\Psi_{2m},\Re,\mathbf{S}_{2m})+\sum_m P(\Psi_{2m+1},\Re,\mathbf{S}_{2m+1}) \tag{6b}$$

and

$$P_B=\sum_m Q(\mathbf{S}'_{2m},\Re,\beta_1)P(\Psi_{2m},\Re,\mathbf{S}'_{2m}) + \sum_m Q(\mathbf{S}'_{2m+1},\Re,\beta_1)P(\Psi_{2m+1},\Re,\mathbf{S}'_{2m+1}), \tag{6c}$$

where the function Q is the spherical wave reflection coefficient for a given source and receiver position and the acoustical characteristics of the plane boundary. Generally speaking, for a given source position $\mathbf{S}$, receiver position $\Re$, and specific normalized admittance of the impedance boundary β, the spherical wave reflection coefficient $Q(\mathbf{S},\Re,\beta)$ can be computed by[23]

$$Q(\mathbf{S},\Re,\beta)=V(\theta)+[1-V(\theta)]F(w), \tag{7a}$$

where the plane wave reflection coefficient $V(\theta)$, the boundary loss factor $F(w)$, and the numerical distance w are determined according to

$$V(\theta)=\frac{\cos\theta-\beta}{\cos\theta+\beta}, \tag{7b}$$

$$F(w)=1+i\sqrt{\pi}we^{-w^2}\,\mathrm{erfc}(-iw), \tag{7c}$$

and

$$w=+\sqrt{\tfrac{1}{2}ikd}(\cos\theta+\beta). \tag{7d}$$

The function erfc(X) is the complementary error function of complex argument X, d is the distance between the image source and receiver, and θ is the angle of incidence of the reflected wave. It is relatively simple to determine d and θ for a given geometrical configuration of the source $\mathbf{S}$ and receiver $\Re$.

Similarly, the total diffracted sound field due to the images of the primary sources Ψ'_n are given below:

$$P'_D=P'_A+P'_B, \tag{8a}$$

where

$$P'_A=\sum_m Q(\Psi'_{2m},\mathbf{S}_{2m},\beta_2)P(\Psi'_{2m},\Re,\mathbf{S}_{2m}) + \sum_m Q(\Psi'_{2m+1},\mathbf{S}_{2m+1},\beta_2)P(\Psi'_{2m+1},\Re,\mathbf{S}_{2m+1}) \tag{8b}$$

and

$$P'_B=\sum_m Q(\mathbf{S}'_{2m},\Re,\beta_1)Q(\Psi'_{2m},\mathbf{S}'_{2m},\beta_2)P(\Psi'_{2m},\Re,\mathbf{S}'_{2m}) + \sum_m Q(\mathbf{S}'_{2m+1},\Re,\beta_1)Q(\Psi'_{2m+1},\mathbf{S}'_{2m+1},\beta_2) \times P(\Psi'_{2m+1},\Re,\mathbf{S}'_{2m+1}). \tag{8c}$$

All series in Eqs. (6b), (6c) and (8b), (8c) start from $m=0$, but the number of terms required in each series is different. It is independent of the source position but depends only on the receiver position between the façade and barrier surfaces.

We need to determine the number of terms required in the series for the calculation of the diffraction fields [cf. Eqs. (6a)–(6c) and (8a)–(8c)]. If the receiver height is less than that of the barrier, as shown in the Region A of Fig. 4, then

multiple reflections between the façade and barrier surfaces are possible, as they are aligned parallel to each other [see also Fig. 3(b)]. Hence, in principle, a sum of infinite diffraction terms is required for each series in Eqs. (6b), (6c) and (8b), (8c). However, in practice, only a finite number of terms are required because the higher-order rays have longer distances to travel between the barrier edge and the receiver. Consequently, higher-order diffracted rays that are smaller in magnitude can be neglected in the total sound field. This could be verified by the convergence of the calculated sound field in the simulations. On the other hand, if the receiver is located at a higher position than the top edge of the barrier, then the number of diffraction terms is dependent on the positions of virtual sources (either $\mathbf{S}_n$ or $\mathbf{S}'_n$) and the receiver $\mathfrak{R}$. This is because multiple reflections between the two surfaces can only be sustained as long as the height of the ray path is less than the top edge of the barrier. As a result, only some diffraction terms from the secondary sources and their images contribute to the total sound field. A close examination of Eqs. (8b) and (8c) reveals that only zeroth- and first-order diffracted rays, $\mathbf{S}_0$ and $\mathbf{S}_1$, can contribute to the total field if the receiver is located in regions B, C, and D, as shown in Fig. 4. Hence, only the first term is required in the series.

To determine the required terms for the series in Eqs. (6c) and (8c), let us consider a pair of consecutive even- and odd-order diffracted rays, $\mathbf{S}'_{2m}$ and $\mathbf{S}'_{2m+1}$, where $m=0,1,2,$ 3, etc. We can easily identify different regions where these two diffracted rays can contribute to the total field. In the $y=0$ plane, a line can be drawn from the virtual source $\mathbf{S}'_{2m}$ to the barrier edge $\mathbf{S}_0$ and its slope can be determined as $-H/mL$. The line can be extended farther until it reaches point M at $(0,0,(m+1)H/m)$ on the façade. By considering the ray path's geometrical configuration, we can see that the diffracted ray can only penetrate Regions A and B in Fig. 4. No diffracted rays from the virtual source $\mathbf{S}'_{2m}$ can reach noise-sensitive receivers that are located at Regions C and D.

The equation of this limiting ray can be determined that leads to the following condition for the receiver position $(x_r,0,z_r)$, where the virtual source $\mathbf{S}'_{2m}$ contributes to the total field,

$$z_r \leqslant -\frac{Hx_r}{mL}+\frac{(m+1)H}{m}. \tag{9}$$

Alternatively, we can determine the maximum number of terms $\hat{m}$ from Eq. (9) as

$$\hat{m}=\mathrm{int}\left[\frac{H(L-x_r)}{L(z_r-H)}\right]. \tag{10}$$

Similarly, there is an analogous limiting ray to determine the region where there is a contribution of the odd-order ray from the virtual source, $\mathbf{S}'_{2m+1}$. We can construct a reflected ray MN, which has a slope of H/mL and passes through the virtual source $\mathbf{S}'_{2m+1}$. It is easy to identify that there is no diffracted ray from the virtual source $\mathbf{S}'_{2m+1}$ in Region D. The corresponding condition for the existence of the diffracted ray is

$$z_r \leqslant \frac{Hx_r}{mL}+\frac{(m+1)H}{m}. \tag{11}$$

In this case, the maximum number of terms $\hat{m}'$ is simply

$$\hat{m}'=\mathrm{int}\left[\frac{H(L+x_r)}{L(z_r-H)}\right]. \tag{12}$$

We remark that further diffraction by the secondary sources and their images, i.e., multiple diffractions at the barrier edge, are ignored in the current formulation. The expression for the diffracted fields can be simplified considerably if the ground surfaces are acoustically hard such that $\beta_1=\beta_2=0$. In this case, all spherical wave reflection coefficients are equal to 1 in Eqs. (6) and (8).

When the receiver height increases above the shadow zone and enters Region II as indicated in Fig. 2(a), the direct line-of-sight contact will be established with the noise source. As a result, the overall sound fields are composed of not only the diffracted wave but also a direct wave and a wave reflected from the façade. Finally, when the receiver height is raised further, only the direct and diffracted waves can reach the receiver [see Region III of Fig. 2(a)]. From the geometrical consideration, the direct line-of-sight sound field P_1 can be written as

$$P_1=\begin{cases} 0, & \text{in Region I,} \\ e^{ikR_a}/4\pi R_a+Q(\Psi_0,\mathfrak{R},\beta_f)e^{ikR_b}/4\pi R_b, & \\ \quad \text{in Region II,} & \\ e^{ikR_a}/4\pi R_a, & \text{in Region III,} \end{cases} \tag{13}$$

where R_a and R_b are, respectively, the pathlengths of the direct wave and the specularly reflected wave on the façade surface.

Similar zones of the sound field can be identified in the vicinity of the barrier due to the image of the primary noise source in the quarter of $x>0$, $z<0$. Three regions of the sound field can be identified, i.e., Regions I′, II′, and III′, as shown in Fig. 2(b). The direct line-of-sight sound field P_2, due to the image of the primary source, can be written analogously as

$$P_2=\begin{cases} 0, & \text{in Region I}', \\ Q(\Psi'_0,\mathfrak{R},\beta_2)[e^{ikR_c}/4\pi R_c+Q(\Psi'_0,\mathfrak{R},\beta_f) & \\ \quad \times e^{ikR_d}/4\pi R_d, & \text{in Region II}', \\ Q(\Psi'_0,\mathfrak{R},\beta_2)e^{ikR_d}/4\pi R_d, & \text{in Region III}', \end{cases} \tag{14}$$

where R_c and R_d are, respectively, the pathlengths of the specularly reflected waves on the ground surface (in the source side) and that reflected on both the ground and façade surfaces.

As can be seen in this section, different regions in the vicinity of a façade–barrier system have different formulas for calculating the sound pressure levels. They have to be identified carefully by considering the geometrical configuration of the barrier, source, and receiver. By incorporating the identified regions in the façade–barrier system from Figs. 1, 2(a), 2(b), and 4, we can compute the sound field P_T in front of a building façade as follows:

$$P_T = P_D + P_D' + P_1 + P_2, \tag{15}$$

where P_D, P_D', P_1, and P_2 can be calculated by Eqs. (6), (8), (13), and (14), respectively. In fact, the region between the façade and barrier is the region of interest because we wish to investigate the effect of the barrier on the change in the overall sound field in front of a tall building.

III. VALIDATION OF THE RAY MODEL

A. Numerical comparisons

The ray model derived in the last section has been implemented for the computation of sound fields in front of a tall building behind a hard screen. A two-dimensional (2-D) Boundary Element Method (BEM) is also used to predict the acoustic sound field of this façade–barrier system. The BEM model is developed and its details of implementation are described elsewhere.[24] As the BEM model is an accurate numerical scheme to handle the scattering and diffraction of sound by obstacles, the predicted results from the BEM model provide useful benchmarking data to validate the ray method. The computational time of a BEM formulation increases with the number of "boundary" elements. As a rule of thumb, six elements per wavelength are required to ensure an acceptable numerical accuracy, although Marburg[25] has pointed out that use of biquadratic or even higher-order boundary elements can lead to a more accurate numerical solution. Obviously, a traffic noise prediction model with a long barrier along the road in front of tall buildings (often over 100 m in height) requires an exceedingly large number of elements, even for a simple 2-D BEM model let alone for the full 3-D model. Nevertheless, to reduce the required computational time, a 2-D BEM model is used in the present paper to obtain the benchmarking results for numerical comparison with the ray model. The use of a 2-D BEM is justifiable because Ouis[26] has showed theoretically that the effect of wave divergence is insignificant such that the 2-D prediction results for a coherent line source are equivalent to a more general 3-D case of a point source. Moreover, the view of Ouis has been supported by scale model[27] and full scale[28] experimental results using point sources.

In this section we present two typical sets of numerical examples for a reflecting screen on a hard ground surface. In this investigation, a realistic outdoor configuration is used in the BEM and ray models. The barrier height is taken to be 3 m and it is situated at 4 m in front of a building façade. We also assume that the contributions from sound diffracted at the top edge of the façade should be negligibly small if the height ratio of façade to barrier is greater than 7:1, i.e., for the height of the façade of about 20 m or more. Obviously, this height ratio is dependent on the frequency range of interest. Using a larger height ratio in the numerical analysis can lead to more accurate BEM results at the expense of a longer computational time. We have no attempt to optimize the height ratio, but the close agreement of numerical comparisons, see Figs. 5 and 6, between the BEM and ray model predictions justifies our choice of the façade height.

The rectangular coordinates, (x,y,z), are used to represent the situation, assuming that the origin (0.0,0.0,0.0) is at the point where the face of the façade meets the ground surface; the top edge of the barrier will be at (4.0,0.0,3.0). The noise source is fixed at a position of 0.3 m high above the hard ground; see Fig. 1 for the general geometrical configuration of the problem. This is used to simulate the engine exhaust noise of a normal vehicle. It is placed 2 m away from the barrier's outer surface, i.e., at point (6.0,0.0,0.3). Four different receiver positions at coordinates of (1.0,0.0,2.0), (1.0,0.0,4.0), (3.0,0.0,2.0), and (3.0,0.0,4.0) are simulated. These receivers are all located within the shadow zone behind the barrier. A frequency range from 100 to 2000 Hz is used in the numerical comparison. Figure 5 displays the results of using the ray model described in Sec. II and the BEM simulation of relative sound pressure levels with the

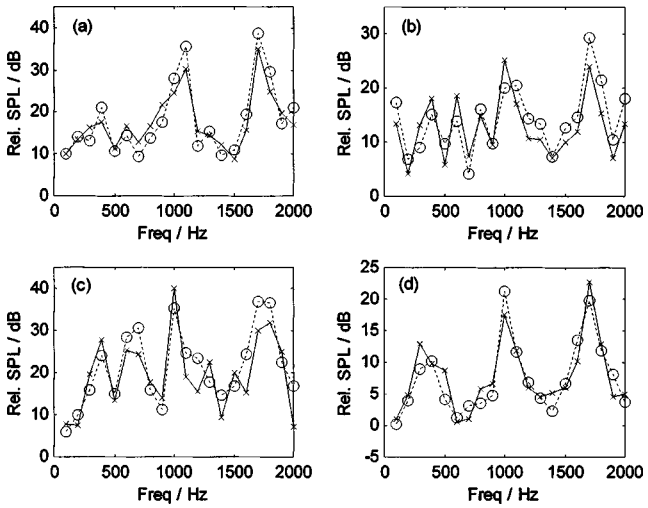

FIG. 5. Theoretical predictions and BEM data for sound propagation of a façade-barrier system. The distance between the building façade and barrier =4.0 m. The barrier height=3.0 m, source height=0.3 m at 2.0 m from the barrier, and the receiver position (the origin is at the base of the barrier where it meets the ground): (a) (1.0,2.0); (b) (1.0,4.0); (c) (3.0,2.0); (d) (3.0,4.0) (dotted line: analytic formulation; solid line: BEM prediction).

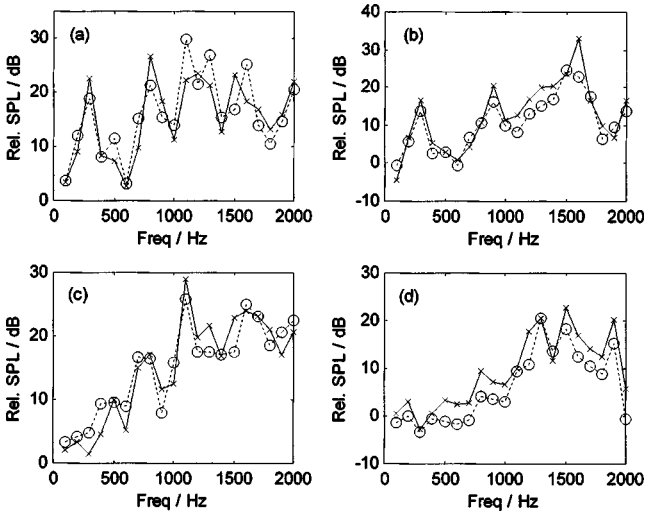

FIG. 6. Theoretical predictions and BEM data for sound propagation of a façade-barrier system. The distance between the building façade and barrier =4.0 m. The barrier height=3.0 m, source height=0.1 m at 4.0 m from the barrier, and the receiver position (the origin is at the base of the barrier where it meets the ground): (a) (1.0,2.0); (b) (1.0,4.0); (c) (3.0,2.0); (d) (3.0,4.0) (dotted line: analytic formulation; solid line: BEM prediction).

reference free-field level. These geometrical configurations are chosen according to the corresponding configuration of the measurement setup shown in the next section. They show good agreement with each other with discrepancies less than 5 dB in general. These discrepancies are due to the numerical deficiency of calculating the BEM data with insufficient ''elements.'' Another simulation is carried out when the source is situated farther away from the barrier surface. It is located 4 m away from the outer barrier's surface and at 0.1 m above the hard ground, i.e., at coordinates (8.0,0.0,0.1). The source can be used to simulate the noise produced near the ground with the interaction with the vehicle. The receivers are kept at the same positions as before between the façade and barrier, i.e., at (1.0,0.0,2.0), (1.0,0.0,4.0), (3.0,0.0,2.0), and (3.0,0.0,4.0). Here, the receivers are located in the shadow and illuminated zones. Figure 6 shows the comparison of the numerical results obtained from the BEM model and the mathematical prediction model developed in the previous section. Again, good agreement between the two curves is achieved with discrepancies less than 5 dB in general. We note that approximately 30 terms are used in the ray model in order to achieve converged results in all predictions shown in Figs. 5 and 6.

B. Experimental validation

The ray model for the prediction of sound pressure levels of the façade–barrier system involves the use of a somewhat intricate set of formulations; cf. Eqs. (1), (13)–(15), which is dependent on the source/receiver position and the relative location of the barrier. To further validate the numerical formulation, indoor experiments were carried out in an anechoic chamber of size 6 m×6 m×4 m. In the measurements, two thin hardwood boards 2 cm thick were used to represent the building façade and barrier surfaces. Both hardwood boards have a nominal width of 2.4 m, but their respective heights are 1.8 and 0.36 m for the simulation of the building façade and the barrier, respectively. The height ratio of the façade to barrier is 5:1 such that we assume the contribution from the sound diffracted at the top edge of the façade does not affect the measured sound fields significantly. Excellent agreements between the experimental results (see Figs. 7 and 8 below) and theoretical predictions justify this assumption.

Two different types of ground surface were simulated in the experiment. Hardwood boards were also used to provide the simulation of a hard ground. All hardwood boards were varnished to create smooth surfaces and were sealed to prevent sound leakage for all measurements. In the experimental measurements, a hard ground was used initially. It was then followed by putting a layer of carpet (about 1 cm thick) on top of the hard ground to create a surface of finite impedance. The barrier base was aligned with the lower face of the carpet. In all experiments, the façade and barrier surfaces were aligned parallel to each other and perpendicular to the ground.

A BSWA TECH MK224 $\frac{1}{2}''$ condenser microphone and a BSWA TECH MA201 preamplifier were used together as the receiver. The microphone was placed between the façade and barrier. A Tannoy driver with a tube with an internal diameter

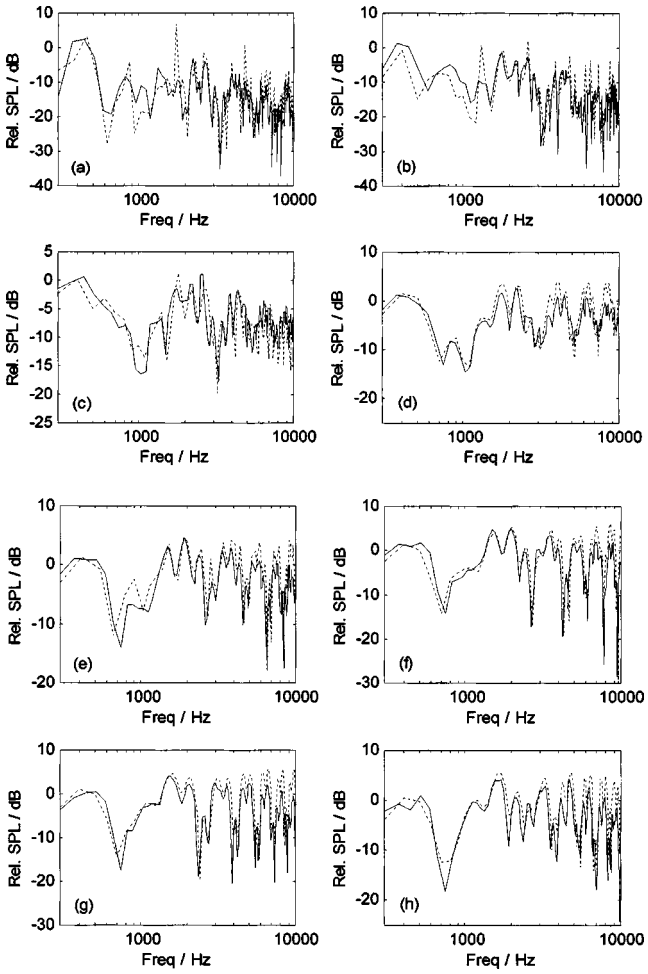

FIG. 7. Experimental data and theoretical predictions for sound propagation of a façade–barrier system. The ground, façade, and barrier are all hard surfaces. The distance between the façade and the barrier=0.79 m. Barrier height=0.36 m. Source height=0.15 m, and the receiver is positioned at 0.395 m from the façade. The height of the receiver from the surface of the ground: (a) 0.2 m; (b) 0.3 m; (c) 0.5 m; (d) 0.6 m; (e) 0.8 m; (f) 0.9 m; (g) 1.0 m; (h) 1.1 m (dotted line: theoretical prediction; solid line: experimental result).

of 3 cm and a length of 1 m was used as a point source in all indoor experiments. The noise source was placed at the opposite side of the barrier. This setup was to simulate the situation in which the barrier was used to protect the noise-sensitive receivers in the building from traffic noise (i.e., to block the line of sight between source and receiver). The Tannoy driver was connected to a maximum length sequence system analyzer (MLSSA) with a MLS card installed in a PC computer.[29] The analyzer was connected to a B&K 2713 amplifier. The MLSSA system was used both as the signal generator for the source and as the signal processing analyzer. The Tannoy driver and the condenser microphone were placed in a fixed position by means of a stand and clamps, and the position of the receiver was adjusted for different sets of measurements. In the experiment, the source and receiver were both located in the same vertical plane mutually perpendicular to the ground and barrier surfaces.

Two sets of experiments were conducted separately above different ground surfaces (hard and carpet-covered). For the hard ground surface, the distance between the façade

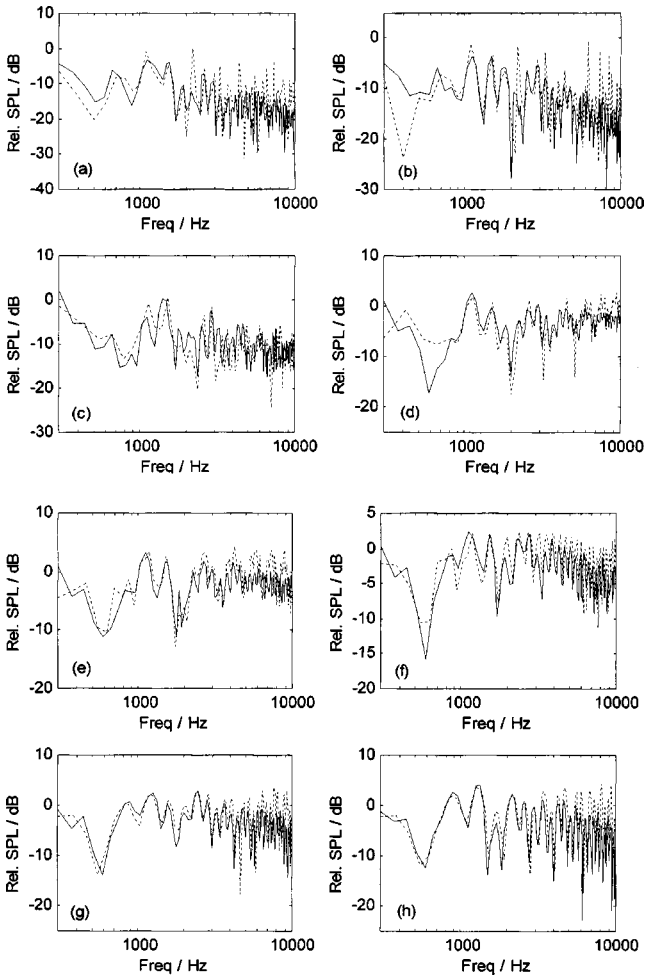

FIG. 8. Experimental data and theoretical predictions for sound propagation of a façade–barrier system. The façade and barrier are of hard surfaces. The hard ground is covered with a layer of carpet. The distance between the façade and the barrier=0.94 m. The barrier height=0.36 m. Source height =0.20 m, and the receiver is positioned at 0.47 m from the façade. The height of the receiver from the surface of the carpet: (a) 0.2 m; (b) 0.3 m; (c) 0.4 m; (d) 0.6 m; (e) 0.7 m; (f) 0.8 m; (g) 0.9 m; (h) 1.1 m (dotted line: theoretical prediction; solid line: experimental result).

and barrier was kept constant at 0.79 m. The receiver was positioned in the middle between these two vertical planes (i.e., 0.395 m from the inner surface of both the façade and barrier). The source height was kept constant at 0.15 m above the ground surface and its distance away from the outer barrier surface was fixed at 0.6 m. The position of the receiver was allowed to vary vertically above the ground surface from 0.2 to 1.1 m. Measurements of the sound field were taken at intervals of 0.1 m. With this geometrical configuration, the receiver position was allowed to vary from locations in the shadow zone to locations in the illumination zone, where direct line-of-sight contact was possible between the source and receiver. Figure 7 displays the experimental results and theoretical predictions of the relative sound pressure levels with the reference free-field level measured at a horizontal distance of 1 m from the source. They both show very good agreement with each other.

For the impedance ground surface, a layer of carpet was put on top of the hardwood board in our indoor experiments. Prior measurements were conducted to characterize the acoustical impedance of the carpet.[30] A two-parameter model[31] was used to predict its effective normalized admittance, as follows:

$$\beta = \frac{1}{0.436(1+i)(\sigma_e/f)^{0.5} + 19.48 i \alpha_e / f}, \tag{16}$$

where σ_e is the effective flow resistivity and α_e is the effective rate of change of porosity with the depth of the material used in the experiment, i.e., carpet. Best-fit parameters with $\sigma_e = 10\,000\ \mathrm{Pa\,s\,m^{-2}}$ and $\alpha_e = 80\ \mathrm{m^{-1}}$ were obtained (see Ref. 30 for typical experimental results of the ground characterization). These paremeter values were used in our subsequent predictions based on the ray method. We remark that Busch *et al.*[32] have reported an improved technique for simultaneously selecting both an optimal scale factor and optimal model materials for indoor scale model experiments. However, there is no attempt to select the most appropriate materials for modeling an outdoor porous ground surface in our present study. However, the use of carpet-covered ground will allow a validation of the ray model by comparing theoretical predictions with precise indoor measurements for ground surfaces with finite impedance.

After the characterization of the ground surface, the second set of experiments was conducted. In these measurements, the separation between the façade and barrier was fixed at 0.94 m. The receiver was placed in the middle between these two vertical planes (i.e., 0.47 m from each of the inner surfaces). The noise source was located on the other side of the barrier. Its position was 0.62 m away from the outer barrier surface and 0.2 m above the carpet covered ground. The position of receiver was raised vertically above the carpet surface from 0.2 to 1.1 m. Experimental results were recorded at 0.1 m intervals. The comparison of the results obtained from the theoretical prediction and experiment is shown in Fig. 8. They show reasonably good agreement for all the measured frequencies. Generally speaking, the developed ray model was able to predict the sound pressure levels in the façade–barrier system.

The total sound pressure levels in the region between the façade and barrier is the summation of the different wave terms produced by the primary and secondary noise sources and their images, as described in Sec. II. For a receiver located below the height of the barrier, the sound pressure level is made up of the multiple reflections of the secondary noise source between the façade and barrier. In this case, it would be ideal to sum up all diffraction terms produced by the secondary source images. In the theoretical prediction using the dimensions of the experimental setup, up to 30 secondary source images are found to be sufficient for predicting the sound pressure levels. However, it should be noted that if the distance between the façade and barrier is very short, a stronger reverberant sound field is formed in the area. Therefore, a large number of secondary source images will be required for the computation. Nevertheless, in a more realistic environment where the distance between the façade and barrier is much greater—of the order of 10 m or more, only a few of these terms are needed for the computation of the total sound field, as higher-order terms are negligibly small. This is due

to the fact that these higher-order terms are weaker in strength when they are located farther from the receiver. Here, we remark that no attempts have been made to explore the effect of absorptive barriers in the current investigations. This area will be an area of future studies.

IV. APPLICATION OF THE RAY MODEL IN URBAN ENVIRONMENTS

With the numerical and experimental validations, we are confident about further applying the ray model to predict the sound field of a façade–barrier system so that we can assess the acoustic performance of a barrier in high-rise cities. Indeed, a barrier aligned parallel to the front of a building is often used to block the noise produced by the traffic on the other side of the barrier. Over the years, it has been proven to be an effective measure. However, little attention has been focused on the distribution of the sound field between the façade and barrier. Therefore, we shall investigate these effects using the ray model described in Sec. II for a variety of source heights and distances away from the barrier.

In the first simulation, the setup of the façade–barrier system is similar to that of Fig. 1. The receiver is placed between the façade and barrier and the source is situated on the other side of the barrier. The source and receiver are located in the same plane in which they are mutually perpendicular to the ground and building façade. The ground, façade, and barrier all have hard and reflecting surfaces. The façade is infinitely high compared with the height of the barrier, and hence the diffraction at the top of the building is ignored. The barrier height is 4 m and is situated 6 m away from the building façade. The source is kept at a distance of 2 m away from the outer barrier's surface (which is the surface facing away from the façade) and its height chosen at 0.5 and 1.5 m above the ground for each simulation.

Figure 9 displays the results of the prediction of the barrier insertion loss. It is calculated as the difference in the A-weighted sound pressure level with and without the presence of the barrier. A white noise spectrum is used for the A-weighting process (see Ref. 31 for details). The region of sound pressure levels in front of the façade of up to 6 m away from its surface and from 0 to 16 m above ground is investigated. The two different heights of noise source considered all obtained a similar range of values of sound pressure level attenuation in the shadow zone from about 0 to 30 dB(A), when the barrier was erected. The most obvious feature of these figures is the variation of the size of the shadow zone behind the barrier. As the position of the source is lifted, the area of the shadow zone on the other side of the barrier decreases. Therefore, people who live on high floors will be protected by the barrier from the noise produced near the ground, such as noise from tires. If the source height is higher, for example, the engine exhaust noise from a large wagon that has the exhaust pipe situated at the top of the truck, the direct line-of-sight contact can be established, even for receivers located at the low to middle floors in a building. The maximum noise attenuation level of about 35 dB(A) is obtained close to the ground behind the barrier when the source is at the lowest position (i.e., 0.5 m). This is because it is easier for the sound waves from the higher source position to travel around and diffract at the top edge of the barrier. Hence, the sound pressure levels attained on the other side of the barrier will be slightly higher compared with the case where the source position is close to the ground. Moreover, the noise attenuation level is higher in the vicinity of the barrier because it is deep inside the shadow zone. As the receiver proceeds toward the façade, the attenuation level becomes less.

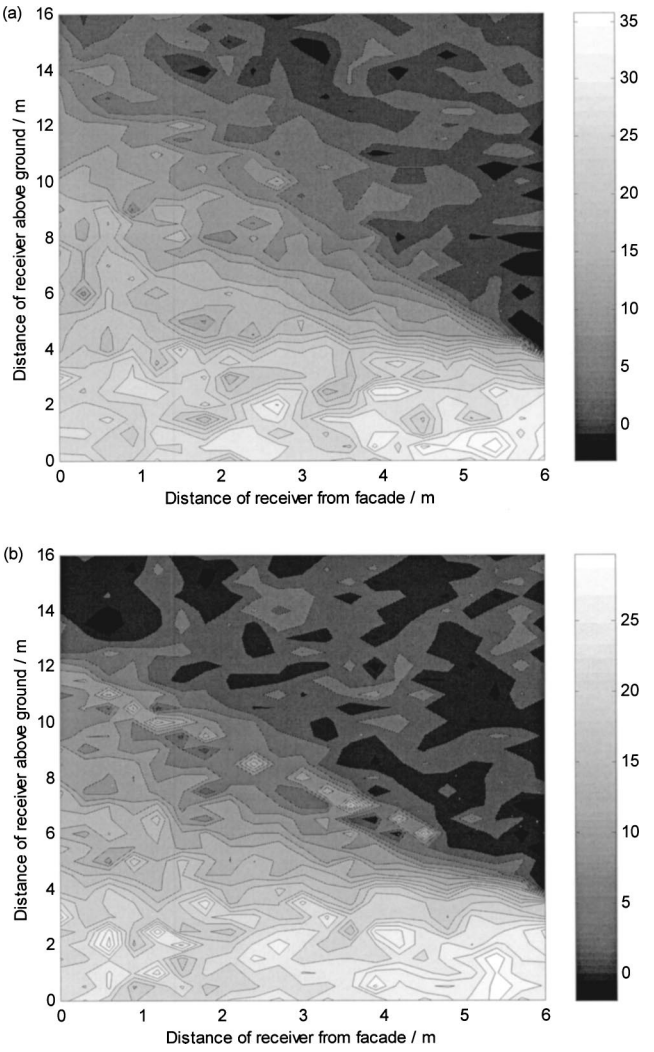

FIG. 9. Prediction of the barrier insertion loss of a façade–barrier system. The façade is erected on the left-hand side. The distance between the façade and the barrier is 6 m. The barrier height is 4 m. The source is located at 2 m from the outer barrier's surface. Source height: (a) 0.5 m; (b) 1.5 m.

Another case is considered for the determination of the sound field of a façade–barrier system when the source is moving away from the barrier. The source is fixed at a height of 0.5 m and its distance away from the outer barrier surface is 2 and 4 m, respectively, for each simulation. Figure 10 shows the prediction of the barrier insertion loss in the same region discussed above (a distance of up to 6 m from the façade surface and from 0 to 16 m above-ground). The two distances considered show similar noise attenuation, from about 0 to 30 dB(A) in the shadow zone, with the presence of a barrier. A slightly higher sound pressure attenuation of 35 dB(A) is found when the source is closest to the barrier at 2 m [Fig. 10(a)]. As expected, the area of the shadow zone

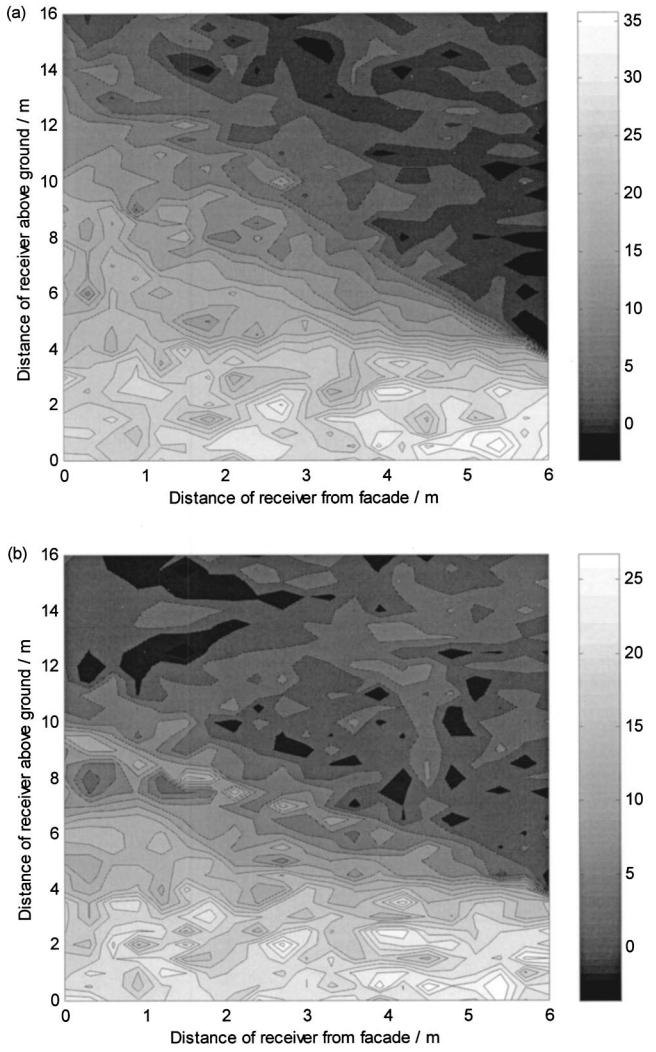

FIG. 10. The prediction of the barrier insertion loss of a façade–barrier system. The façade is erected on the left-hand side. The distance between the façade and the barrier is 6 m. The barrier height is 4 m. The source height is situated at 0.5 m above the ground, and at (a) 2.0 m; (b) 4.0 m from the outer barrier's surface.

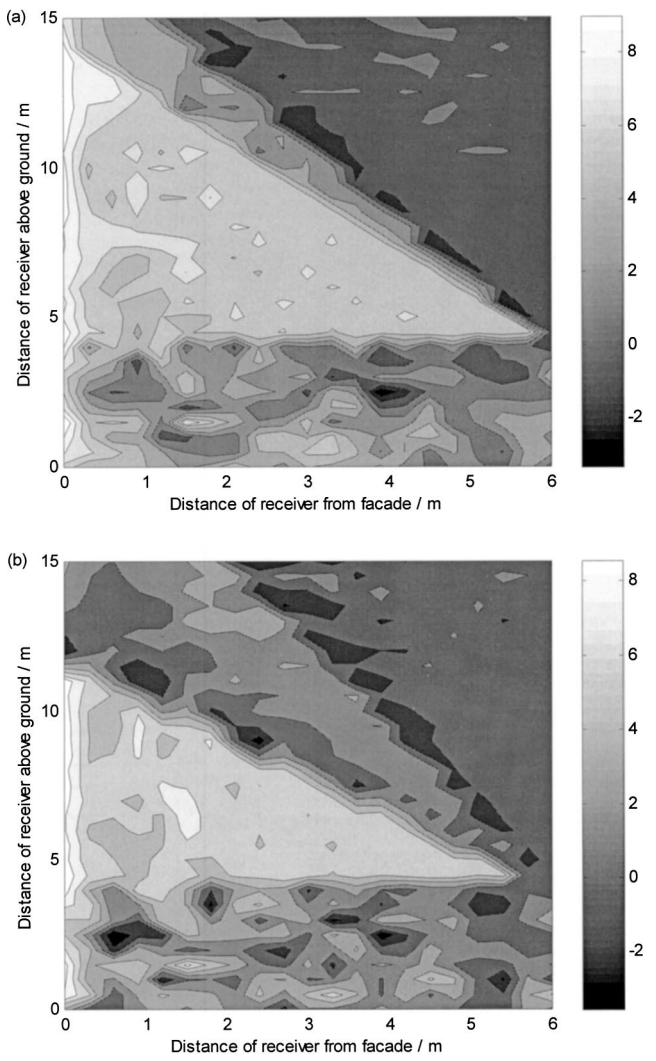

FIG. 11. The prediction of the insertion loss degradation of the building façade in a façade–barrier system. The barrier is erected on the right-hand side. The configuration of the noise source, receiver, barrier, and façade is the same as described in the setup in Fig. 9.

behind the barrier diminishes with an increase in the distance of source away from the barrier. Again, better noise attenuation is found close to the barrier and ground surface, i.e., deep inside the shadow zone. Therefore, the residents on higher floors are better protected by the barrier when traffic is operating close to it.

The presence of a building next to a road leads to the reflection of noise on the façade's surface. It was shown earlier in this section that the insertion of a barrier creates a shadow zone that can protect the residents of low to middle floors from traffic noise. In the region close to the ground [region I in Fig. 2(a)], multiple reflections of the diffracted sound occur between the façade and barrier. Above the height of the barrier within region I, diffracted sound waves impinge on the façade and barrier surfaces before reaching the receiver. Above the shadow zone, direct, reflected, and diffracted sound waves contribute to the total sound field. The presence of a building façade seems to be rather significant in determining the sound fields in front of it because of its nature to reflect noise. Here, we investigate the effects of the sound pressure levels behind a barrier due to the presence of a tall building, i.e., the insertion loss degradation[20] of the building façade. The insertion loss degradation (DIL) represents the difference in sound pressure levels before and after the erection of the building. It can be calculated using Eq. (13):

$$\mathrm{DIL} = 20 \log \left| \frac{P_{\text{total,ground+barrier}}}{P_{\text{total,ground+facade+barriers}}} \right|. \tag{17}$$

Two simulations are considered to predict the insertion loss degradation of a building façade (assumed to be infinitely high) behind a barrier. A barrier of 4 m high is aligned parallel at 10 m in front of a building. A noise source is fixed at 2 m from the outer barrier's surface. The receiver position varies inside the region between the façade and barrier, that is, 0–6 m from the inner barrier surface and 0–15 m above the hard ground. In the first simulation, the configuration of the noise source, receiver, barrier, and building façade is the same as the setup described in Fig. 9. The two contour plots in Fig. 11 show the insertion loss degradation of the building façade, when the noise source is 0.5 and 1.5 m above the

hard ground, respectively. This is calculated as the difference in the A-weighted sound pressure levels with and without the consideration of the building façade. The range of the overall insertion loss degradation is from about −6 to 8 dB(A). Positive readings indicate an increase in the sound pressure levels due to insertion of the building façade. From the two plots shown in Fig. 11, the maximum degradation occurs near the façade surface within the shadow zone. A receiver situated in the region above the height of the barrier and inside the shadow zone also experiences quite a large insertion loss degradation of about 5 to 8 dB(A), in general. The area of this insertion loss degradation is inversely proportional to the height of the noise source. Furthermore, the magnitude of the degradation is slightly more apparent when the position of the noise source is high. Hence, a noisier environment is created above the level of barrier. In the region close to the ground, the change in insertion loss degradation is smaller. It ranges from about −2 to 3 dB(A), which indicates that the increase in sound pressure levels due to the multiple reflections of sound between the façade and barrier is not too significant. At some positions, especially near the barrier, a negative insertion loss degradation is found. This implies that the presence of the building leads to a quieter environment at those locations.

In the region above the shadow zone, there is almost no change in the insertion loss degradation, whether or not the building is erected. This indicates that the direct line of sight between the source and receiver is dominant in the overall sound field. A more negative insertion loss degradation is found just above the shadow zone. The variation of the sound field is due to the interference effects between the diffracted waves at the barrier's top edge and the reflected waves from the façade's surface. It is noteworthy that significant variability in the barrier insertion loss over short spatial scales is evident in Figs. 9–11. This is an artifact of the calculation method. The contours in these figures will have smoother appearance if more points are used in the designated regions or more frequencies had been used in the calculations.

V. CONCLUSIONS

Our aim in the present study is to investigate the acoustical performance of noise barriers in a high-rise city. A ray model was developed for a barrier placed closed to high-rise buildings in many urban areas. The ray model was validated by extensive numerical studies and precise indoor experimental measurments. Simulations of sound fields were then carried out for different configurations in typical urban environments. In particular, the sound field in the vicinity of a façade–barrier system was investigated in which a barrier was aligned parallel to the front of a building. The receiver was positioned between the building façade and the barrier and a noise source was situated on the other side of the barrier. The secondary noise source was formed at the top edge of the barrier due to the diffraction at this position. A series of secondary source images were formed due to the multiple reflections between the façade and barrier. The sound pressure levels obtained by the receiver when it is below the top edge of the barrier consists of the summation of the diffracted sound waves of the secondary source images. When the receiver is lifted up to a position above the shadow zone of the barrier, the direct sound wave from the noise source to the receiver and/or noise reflection from the ground surface may be established. Different regions of the sound field can be identified in the vicinity of the façade–barrier system. The size and position of these regions are dependent on the configuration of the barrier, source, and receiver.

In predicting the insertion loss of a noise barrier, the maximum noise attenuation is obtained close to the ground immediately behind the barrier, deep within the shadow zone. In general, slightly less attenuation of the noise is found when the receiver is close to the building façade. The erection of a barrier close to the traffic has a significant effect for the people who live on the higher floors of a building. The effect is greatest for noise produced close to the ground, such as tire noise, as this creates a bigger shadow zone behind the barrier.

The presence of a building façade behind a noise barrier causes an increase in sound pressure levels in the region between these two vertical planes, especially close to the façade surface and above the barrier's top edge within the shadow zone. When a receiver is close to the ground, multiple reflections, which take place between the façade and barrier, lead to an increase in the sound field. The effect due to reflection on the façade surface also increases the sound pressure levels in the region within the shadow. However, above the shadow zone region, the change in sound pressure levels is not significant because of the domination of the direct sound waves.

ACKNOWLEDGMENTS

This research was supported in part by the Research Grants Council of the Hong Kong Special Administrative Region (Project No. PolyU 5151/99E) and the Hong Kong Polytechnic University. The financial support of the Research Committee of the Hong Kong Polytechnic University is gratefully acknowledged for the award of a Research Studentship to one of the authors (S.H.T.). The manuscript was prepared while K.M.L. was on a study leave at the Department of Mechanical, Materials, and Mechatronics Engineering, The University of Western Australia (UWA). One of the authors (K.M.L.) wishes to thank Dr. Jie Pan (UWA), Professor W. S. Siu (PolyU), and Professor R. M. C. So (PolyU) for the opportunity to visit UWA.

[1] R. H. Bolt and E. A. G. Shaw, "Initial program of the Co-ordinating Committee on environmental acoustics," J. Acoust. Soc. Am. **50**, 443–445 (1971).
[2] W. E. Scholes, "Noise reduction by barriers," Proceedings of the British Acoustics Society Meeting, Paper 70/67, April 1970.
[3] U. J. Kurze and G. S. Anderson, "Sound attenuation by barriers," Appl. Acoust. **4**, 35–53 (1971).
[4] Z. Maekawa, K. Fujiwara, and M. Morimoto, "Some problems of noise reduction by barriers," *Symposium On Noise Prevention*, Miskolc, Paper No. 4.8, 1971.
[5] U. J. Kurze, "Noise reduction by barriers," J. Acoust. Soc. Am. **55**, 504–518 (1974).
[6] A. D. Pierce, "Diffraction of sound around corners and over wide barriers," J. Acoust. Soc. Am. **55**, 941–944 (1974).

[7] Z. Mawkawa, ''Noise reduction by screens,'' Appl. Acoust. **1**, 157–173 (1968).
[8] S. Hayek, ''Mathematical modeling of absorbent highway noise barriers,'' Appl. Acoust. **31**, 77–100 (1990).
[9] J. J. Bowman, T. B. A. Senior, and P. L. E. Uslenghi, *Electromagnetic and Acoustic Scattering by Simple Shapes* (North-Holland, Amsterdam, 1969).
[10] J. Nicolas, T. F. W. Embleton, and J. E. Piercy, ''Precise model measurements versus theoretical prediction of barrier insertion loss in the present of the ground,'' J. Acoust. Soc. Am. **73**, 44–54 (1983).
[11] A. L'Espérance, J. Nicolas, and G. A. Daigle, ''Insertion loss of absorbent barriers on ground,'' J. Acoust. Soc. Am. **86**, 1060–1064 (1989).
[12] E. M. Salomons, A. C. Geerlings, and D. Duhamel, ''Comparison of a ray model and a Fourier-Boundary Element Method for traffic noise situations with multiple diffractions and reflections,'' Acustica **83**, 35–47 (1997).
[13] Department of Transport and Welsh Office, *Calculation of Road Traffic Noise*, HMSO, 1988.
[14] T. M. Barry and J. A. Reagan, FHWA Highway Traffic Noise Prediction Model, U.S. Federal Highway Administration, Report FHWA-RD-7-108, Washington, DC, 1978.
[15] Y. Sakurai, E. Walerian, and H. Morimoto, ''Noise barrier for a building façade,'' J. Acoust. Soc. Jpn. (E) **11**, 257–265 (1990).
[16] E. Walerian, R. Janczur, and M. Czechowicz, ''Sound levels forecasting for city-centers. Part I: Sound level due to a road within an urban canyon,'' Appl. Acoust. **62**, 359–380 (2001).
[17] W. F. Cheng and C. F. Ng, ''The acoustic performance of an inclined barrier for high-rise residents,'' J. Sound Vib. **242**, 295–308 (2001).
[18] L. Godinho, J. Antonio, and A. Tadeu, ''3D sound scattering by rigid barriers in the vicinity of tall buildings,'' Appl. Acoust. **62**, 1229–1248 (2001).
[19] L. L. Beranek and I. L. Ver, *Noise and Vibration Control Engineering* (Wiley Interscience, New York, 1992).
[20] R. Panneton, A. L'Espérance, and G. A. Daigle, ''Development and validation of a model predicting the performance of hard or absorbent parallel noise barriers,'' J. Acoust. Soc. Jpn. (E) **14**, 251–258 (1993).
[21] W. J. Hadden and A. D. Pierce, ''Diffraction of sound around corners and over wide barriers,'' J. Acoust. Soc. Am. **69**, 1266–1276 (1981).
[22] M. Abramowitz and A. Stegun, *Handbook of Mathematical Functions with Formulas, Graphs, and Mathematical Tables* (Dover, New York, 1970), Chap. 7, p. 300.
[23] K. Attenborough, ''Review of ground effects on outdoor sound propagation from continuous broadband sources,'' Appl. Acoust. **24**, 289–319 (1988).
[24] G. R. Watt, S. N. Chandler-Wilde, and P. A. Morgan, ''The combined effects of porous asphalt surfacing and barriers on traffic noise,'' Appl. Acoust. **58**, 351–377 (1999).
[25] S. Marburg, ''Six boundary elements per wavelength: Is that enough?'' J. Comput. Acoust. **10**, 25–51 (2002).
[26] D. Ouis, ''Noise shielding by simple barriers: Comparison between the performance of spherical and line sound sources,'' J. Comput. Acoust. **8**, 25–51 (2000).
[27] D. C. Hothersall, S. N. Chandler-Wilde, and N. M. Hajmirzae, ''Efficiency of single noise barriers,'' J. Sound Vib. **146**, 303–321 (1991).
[28] G. R. Watt, D. H. Crombie, and D. C. Hothersall, ''Acoustic performance of new designs of traffic noise barriers: full scale tests,'' J. Sound Vib. **177**, 289–305 (1994).
[29] D. D. Rife and J. Vanderkooy, ''Transfer-function measurement with maximum length sequences,'' J. Audio Eng. Soc. **37**, 419–444 (1989).
[30] S. H. Tang and K. M. Li, ''The prediction of façade effects from a point source above an impedance ground,'' J. Acoust. Soc. Am. **110**, 278–288 (2001).
[31] K. Attenborough, ''Ground parameter information for propagation modelling,'' J. Acoust. Soc. Am. **92**, 418–427 (1992).
[32] T. A. Busch and M. R. Hodgson, ''Improved method for selecting scale factors and model materials for scale modeling of outdoor sound propagation,'' J. Sound Vib. **243**, 173–181 (2001).